



Mechanical and dynamic properties of nettle-polyester composite

Nataraj Mahendrakumar^{1,*}, Pudukarai Ramaswamy Thyla¹, Pidugun Venkatachalam Mohanram², Aruchamy Sabareeswaran¹, Ranjan Biswal Manas¹, and Sridhar Srivatsan¹

¹Department of Mechanical Engineering, PSG College of Technology, Peelamedu, Coimbatore 641004, India

²Department of Mechanical Engineering, PSG Institute of Technology and Applied Research, Neelambur, Coimbatore 641062, India

ABSTRACT

This work deals with the use of Himalayan Nettle (a natural plant fiber) as a reinforcement in polyester resin matrix and characterisation of as-formed nettle-polyester composite. Tensile test on single nettle fibers revealed that the Young's modulus and tensile strength decrease with increase in fiber diameter, and chemical composition test results show that the fiber has higher content of cellulose, hemi-cellulose and lignin that result in better mechanical, biodegrading and thermal stability properties of the composite respectively. Characterization of mechanical properties of randomly-oriented short himalayan nettle fiber reinforced-polyester resin matrix composite was done using tensile, compression and flexural test results. New analytical models were developed considering the effects of orientation and variation of fiber diameters for the determination of Young's modulus and tensile strength. The models are found to yield results which are in good correlation with experimental results. Experimental modal analysis was carried out on cantilever beam specimens for determining material and material plus structural damping ratios using half power band-width method. At higher frequencies, the average damping ratios were found to be 4 to 10 times higher than polymer concrete, C.I. and steel materials. Morphological analysis of the composite (SEM) revealed the structure of the nettle fiber to be hollow, which helps to improve specific stiffness and vibration absorption ability.

Keywords: Natural Fiber-Nettle, Polymer Matrix-Polyester, Mechanical Properties, Natural Frequency, Damping Ratio.

1. INTRODUCTION

One of the parameters that is being studied and researched today in the field of machine tools is the reduction of weight without sacrificing structural properties such as stiffness and damping. High structural stiffness and damping are desired properties in machine tool applications, as they lead to higher cutting speeds which improve productivity (by reducing the cycle time). The conventional machine tool materials have either high stiffness or high damping capacity but suffer from a

major disadvantage of low strength to weight ratio. Composite materials help to overcome the disadvantage of conventional machine tool materials. The light weight properties of natural fiber composites have been found to result in improved specific stiffness and damping properties which will aid in enhancing the operating speed in machine tool applications. Further, natural fiber production and processing has lower adverse environmental impact and energy requirement compared to synthetic fiber production. Natural fiber composites need higher fiber content for achieving performance equivalent to synthetic fibers, thus reducing the more polluting polymer content in composite.

* Author to whom correspondence should be addressed.
Email: nmahendranet@gmail.com

Rowell et al.⁽¹⁾ studied kenaf–polypropylene composite and reported the tensile modulus and strength as 8.3 GPa and 65 MPa respectively. Mohanty et al.⁽²⁾ discussed sustainable bio-composites synthesized from renewable resources, classified the natural/bio fibers and concluded that the main advantage of the bio-composite was high specific stiffness and excellent sound absorption efficiency. Summerscales et al.⁽³⁾ state that hemp, flax, jute and kenaf based thermoplastic matrix composites could be used to build internal and external structures in automotive applications and reported aircraft panels, gear wheels and other machine parts being manufactured using strong high grade paper by nettle fiber reinforcing plastic. The same was experimented by Britain's Ministry of Aircraft Production unit during the Second World War. Nishino et al.⁽⁴⁾ studied kenaf–polymer composite and reported a Young's modulus of 6.4 GPa, tensile strength of 60 MPa (for a volume fraction of 70% fiber, 30% resin). Ochi⁽⁵⁾ obtained 223 MPa as tensile strength and 254 MPa as flexural strength in kenaf reinforced PLA composites. Koichi et al.⁽⁶⁾ reported that the ramie fiber was alkali treated by 15% NaOH which improved tensile strength by 4–18% (661 MPa) compared to untreated ramie fiber (560 MPa) due to changes in microfibrillar angles. Fracture strains drastically increased 2–3 times with a decrease in the microfibrils and with the removal of binding materials around the microfibrils during mercerization. Bodros and Baley⁽⁷⁾ studied and analysed the tensile properties of urtica nettle fibers and reported the average Young's modulus and tensile properties. Young's modulus equal to 87 GPa (± 2.8) and tensile strength equal to 1594 MPa (± 640) and a strain at failure equal to 2.11% (± 0.83) were reported. They also suggested this fiber to be suitable for structural composite manufacturing they also found that Young's modulus decreased with increasing fiber diameter. Singha and Vijay Kumar Thakur⁽⁸⁾ revealed the mechanical properties of hibiscus sabdariffa fiber as reinforcing material in urea-formaldehyde resin matrix and found that particle reinforced composite have a lesser wear rate than short and long fiber reinforced composite. Xie et al.⁽⁹⁾ concluded that the silane treatment of the fiber increases interfacial adhesion between fiber and polymer which increased the mechanical properties of the composite. Athijayamani et al.⁽¹⁰⁾ analysed roselle and sisal natural fiber reinforced polyester composite; the hybrid fiber reinforced polyester composite was prepared based on the fiber content in weight (%) and length of the fibers used. It was reported that, by increasing the fiber content to 30% where the length of the fiber was 150 mm in 70% resin, the composite exhibited increased tensile strength of 58.7 MPa and also increased flexural strength of 76.5 MPa but the impact strength was found to decrease 1.32 kJ/m².

The main focus of this research is to develop a new natural fiber composite for machine tool applications to enhance the static and dynamic performance

of the machine tool with low energy consumption and cost. In this study, mechanical and dynamic properties of a newly-developed randomly oriented, short Himalayan nettle-polyester composite were studied. At first, the morphological, mechanical and chemical properties of the himalayan nettle fiber were investigated. Steel dies were developed to manufacture composite specimens of required volume fractions for different mechanical tests as per ASTM standards. Tensile, compressive, flexural and damping (material and material plus structural) tests were carried out on the composite specimens. A new analytical model was developed for tensile modulus and strength of the composite considering the effects of fiber orientation and variation in fiber diameters. The analytical results were compared with experimental results. Finally, post-testing, the results are discussed and conclusions are presented.

2. EXPERIMENTAL DETAILS

2.1. Fiber Properties

The Himalayan nettle (*Girardinia heterophylla*) fiber studied was procured from Uttarakhand Bamboo and Fiber Development Board; India (cost Rs. 400/kg). It is found to be hollow in nature. The mechanical properties of bast fibers, such as tensile strength and modulus of elasticity are related to the composition, and the external and internal structures of the fibers. The external structure of the fiber has different cross-sectional geometry and also contains many defects along the length, which may affect the mechanical properties. Nettle fiber was pre-treated by immersing the fibers in sodium hydroxide (NaOH) (6–10%) aqueous solution for a period of 24 hours and dried; this modifies the surface roughness of the external surface of the fiber before introduction into polymer matrix and hence results in improved mechanical properties through better binding effect.⁽¹¹⁾

2.1.1. Mechanical Properties

The cross section of the fiber is assumed as circular and its diameter is not constant along the length. Investigations were carried out on 90 samples of himalayan nettle (*Girardinia heterophylla*) fiber to determine mechanical (effective Young's modulus and tensile strength) properties versus diameter. Fiber mean diameters (outer and inner) are calculated from the measurement of diameters at multiple linear positions along their length by optical microscopy. Ten distinct classes *i* were formed based on fiber outside diameters ranging from 50 to 150 μm , with a class interval of 10 μm . Tensile test was carried out on a computerized (Zwick-Roell) universal testing machine (100 N load cell) as per ASTM D3822 for different diameters of fibers at standard laboratory atmosphere (23 °C \pm 3 °C and 50 \pm 10% relative humidity). Each fiber was clamped using wedge grips at a grip length of 37.5 mm on each side. A gauge length of 25 mm and cross head speed of 2.5 mm/min were used for effective Young's modulus

measurement and the results are summarised in Table I, where n_i -number of fibers in each class i , do_i and di_i -mean outer and inner diameters in each class i , E_i and σ_i -mean Young's modulus and tensile strength of fiber in each class i respectively. The Young's modulus E_i and tensile strength σ_i depend on fiber diameters (do_i , di_i) and are found to decrease with increase in fiber diameter. The same trend was observed in flax fibers.⁽¹²⁾ Equation (1) represents the longitudinal Young's modulus of a unidirectional fiber composite material proposed by Lamy and Baley.⁽¹²⁾

$$E_c = \sum_{i=1}^n V_{fi} \times E_i + (1 - V_f) \times E_m \quad (1)$$

where i is the class number, V_{fi} is the volume fraction of fibers with outer and inner diameters do_i and di_i respectively and is proportional to the cross section of fibres i and hence to $n_i \times 0.55do_i^2$ derived from diametrical ratios (D_{ri}) which is found to be equal to 1.5 and are represented in Eqs. (2) and (3), E_m is the Young's modulus of the matrix; V_f is the total volume fraction of fibers denoted in Eq. (4).

$$D_{ri} = \frac{do_i}{di_i} = 1.5 \quad (2)$$

$$do_i^2 - di_i^2 = 0.55 do_i^2 \quad (3)$$

$$V_f = \sum_{i=1}^n V_{fi} \quad (4)$$

The first term in Eq. (1) can be expressed as follows

$$\sum_{i=1}^n V_{fi} \times E_i = V_f \times \sum_{i=1}^n \frac{V_{fi}}{V_f} E_i = V_f \times \sum_{i=1}^n \frac{n_i \times 0.55do_i^2}{\sum_{i=1}^n n_i \times 0.55do_i^2} E_i \quad (5)$$

Equations (6) and (7) represent the contribution of Young's modulus and tensile strength of fibers of class n_i (mean diameter do_i and di_i) to the Young's modulus (E_f) and tensile strength (σ_f) and the same are denoted by K_i and S_i respectively. Values of these contributions are given in Table I.

$$K_i = \frac{n_i \times 0.55do_i^2}{\sum_{i=1}^n n_i \times 0.55do_i^2} \times E_i \quad (6)$$

$$S_i = \frac{n_i \times 0.55do_i^2}{\sum_{i=1}^n n_i \times 0.55do_i^2} \times \sigma_i \quad (7)$$

The following expressions represents the summed value of E_f and σ_f ,

$$E_f = \sum_{i=1}^n \frac{n_i \times 0.55do_i^2}{\sum_{i=1}^n n_i \times 0.55do_i^2} E_i \quad (8)$$

$$\sigma_f = \sum_{i=1}^n \frac{n_i \times 0.55do_i^2}{\sum_{i=1}^n n_i \times 0.55do_i^2} \sigma_i \quad (9)$$

For the sample of fibers tested, the summed value of Young's modulus and tensile strength were calculated as $E_f = 62$ GPa and $\sigma_f = 86$ MPa respectively using the Eqs. (8) and (9). From Eqs. (10) and (11) it can be seen that 30% of fibers (from classes 8 to 10) contribute to 50% and 47% of the summed modulus E_f and tensile strength σ_f of fibers respectively.

$$\sum_{i=8}^{10} K_i = 50\% E_f \quad (10)$$

$$\sum_{i=8}^{10} S_i = 47\% \sigma_f \quad (11)$$

Hence, by proper selection of fiber diameters, the elastic properties of the randomly oriented short nettle fiber reinforced polyester composite can be improved.

2.1.2. Chemical Properties

High degree of polymerization and low microfibrillar angles result in improved mechanical properties in natural fibers.⁽¹²⁾ Microfibrils angles strongly influence the mechanical properties of the fibers. Similarly they are also influenced by the type of cellulose. Each type of cellulose has its own cell geometry. The natural fiber has higher content of cellulose which yields better mechanical properties, similarly hemi-cellulose and lignin influences biodegrading and thermal stability of the composite. The chemical properties of the fibers were tested and the observations are presented in Table II. The results clearly show that himalayan nettle has properties similar to other natural stinging nettle fiber.⁽¹³⁾ The density of the himalayan nettle fiber was found to be 1250 kg/m³, while the density of stinging nettle fiber is 1510 kg/m³⁽¹³⁾ and hence it is

Table I. Sample of himalayan nettle fibers, values n_i , do_i , E_i , σ_i , ϵ_i , V_{fi} , K_i , and S_i .

Class i	1	2	3	4	5	6	7	8	9	10
n_i	7	10	12	7	10	5	12	10	8	9
do_i	54.190	64.483	72.243	84.405	94.942	106.708	114.009	126.915	135.577	145.646
di_i	36.595	43.403	50.499	56.526	63.442	71.150	75.924	84.350	88.693	96.551
$D_{ri} = do_i/di_i$	1.5	1.5	1.4	1.5	1.5	1.5	1.5	1.5	1.5	1.5
E_i	75.3	70.0	67.7	62.5	62.3	61.6	61.3	61.1	60.7	60.3
σ_i	100.0	99.2	97.5	92.9	92.6	87.6	86.6	83.0	80.0	78.9
ϵ_i	2.7	2.6	2.6	2.5	2.5	2.3	2.1	2.0	1.9	1.8
$V_{fi} = n_i \times 0.55do_i^2$	11306	22869	34446	27428	49577	31313	85787	88591	80877	105003
K_i	1.584	2.980	4.338	3.190	5.750	3.588	9.793	10.075	9.134	11.780
S_i	2.546	4.751	6.798	4.761	8.559	5.052	13.633	13.441	11.745	14.938
										$E_f = 62$
										$\sigma_f = 86$

Table II. Properties of himalayan nettle fiber (*Girardinia heterophylla*).

Diameter (μm)	50–150
Density (g/cm^3)	1.25
Cellulose (%)	85.93
Hemicellulose (%)	6.8
Lignin (%)	5.49
Waxes (%)	0.08
Elongation at breaks (%)	2
Tensile strength (MPa)	86
Young's modulus (GPa)	62

clear that himalayan nettle has lower density. Hence for the same geometrical parameters, the natural fiber shows higher specific stiffness.⁽¹⁴⁾ The density of the natural fibers is half that of the synthetic fibers.

2.2. Matrix Properties

Table III shows typical properties of unsaturated polyester resin matrix as supplied by MNP chemicals, India (cost Rs. 150/kg). It has good mechanical, impact and wear resistance properties. Thus, the polyester resin matrix selected is a good candidate for the chosen composite application.

For the characterization of the mechanical and dynamic properties as per ASTM standards, tensile (D3039, $250 \times 25 \times 2.5$ mm), compression (D695, $25.4 \times 25.4 \times 25.4$ mm), flexural (D6272, $127 \times 12.7 \times 3.2$ mm) and cantilever beam specimens ($500 \times 25 \times 15$ mm) of the composite consisting of randomly oriented short nettle fiber and polyester resin was prepared using compression moulding technique at a pressure of 1 MPa (10 bar) and room temperature. Prior to compression moulding the fiber was stored at ($23 \text{ }^\circ\text{C} \pm 2 \text{ }^\circ\text{C}$ and $50 \pm 5\%$ relative humidity) for a period of 40 hours. The mixing ratio by volume fraction of short nettle-fiber and polyester-resin was chosen as 38% and 62% respectively for manufacturing the nettle-polyester composite. This ratio was arrived at based on preliminary experimental investigations on strength and fiber-resin binding. The fibers were cut to 25 mm length for better fiber dispersion, effective reinforcement and stress transfer in polyester matrix.⁽¹⁵⁾ The fibres were then weighed and kept in a tray, and 250 grams of polyester resin was added with 2% (i.e., 5 g) accelerator and then 2% (5 g) catalyst in a beaker and were stirred till a homogeneous mixture was obtained.

Table III. Properties of polyester matrix [product of literature].

Appearance	Pale yellow colour
Viscosity (cps)	650
Density (g/cm^3)	1.15
Elongation at breaks (%)	4.8
Tensile strength (MPa)	41 ± 1.6
Young's modulus (GPa)	1 ± 0.004
Flexural strength (MPa)	61 ± 2.26
Flexural modulus (MPa)	2.2461 ± 0.0022
Poisson's ratio	0.38

The die fabricated for compression moulding process consists of two halves, namely, top and bottom mould. The same die can be used to make different specimens as per ASTM standards by adjusting the height of the top mould punch. Mild steel and EN 24 were used as materials for the fabrication of the modular die. Another mild steel die was used to make cantilever beam specimens for the determination of natural frequency and damping ratio of the composite.

2.3. Molding and Machining

Using standard tools, the moulds were prepared and then mould release agent wax and PVOH (Polyvinyl Alcohol) were applied over the steel die surfaces for facilitating the removal of specimens. Using a measuring jar, 2.5 ml of the matrix mix was poured onto the bottom of the mould. Then the first layer of short nettle fiber was placed randomly over the added mix. An additional 2.5 ml of mix was added over the nettle fiber layer that had been already placed in the die and the second layer of fiber was placed over the matrix mix. The procedure was repeated till the mould cavity was filled with composite material. Now the top and bottom mould cavities were fitted on to the top and bottom platens of the compression moulding machine. The mould was closed and pressed at 1 MPa (10 bar) pressure at room temperature.⁽¹⁵⁾ Due to exothermic reaction, the temperature of the mould increased up to $80\text{--}100 \text{ }^\circ\text{C}$. After the composite was cured, the mould was opened carefully and the composite sample was removed.

The moulded specimens were machined by using milling and grinding machines to achieve dimensions of the standard specimen. The sequences of machining operations employed are edge milling to ensure that the composite specimen is free from cracks and dents in both the edges, flat surface grinding to maintain parallelism and thickness of the composite specimen and finally the specimen length, width and thickness dimensions were inspected to ensure conformity with ASTM standards.

2.4. Morphology Analysis

Images were taken with scanning electron microscope (SEM) for making morphological study of the composite. This helped in the study of dynamic properties and failure mechanisms of the composite. SEM image in Figure 1(a) shows the strong bond formation between nettle fiber and polyester matrix. This strongly influences better load transfer from matrix to short fiber from one end to the other end which will lead to better performance. The important modification done by alkaline treatment is the disruption of hydrogen bonding in the network structure, thereby increasing surface roughness.⁽¹⁶⁾ The pretreatment of nettle fiber in (6–10%) aqueous solution of NaOH resulted in the removal of lignin and hemicelluloses from the fiber surface. This improved outer surface roughness, results in enhancement of aspect ratio which helps to obtain

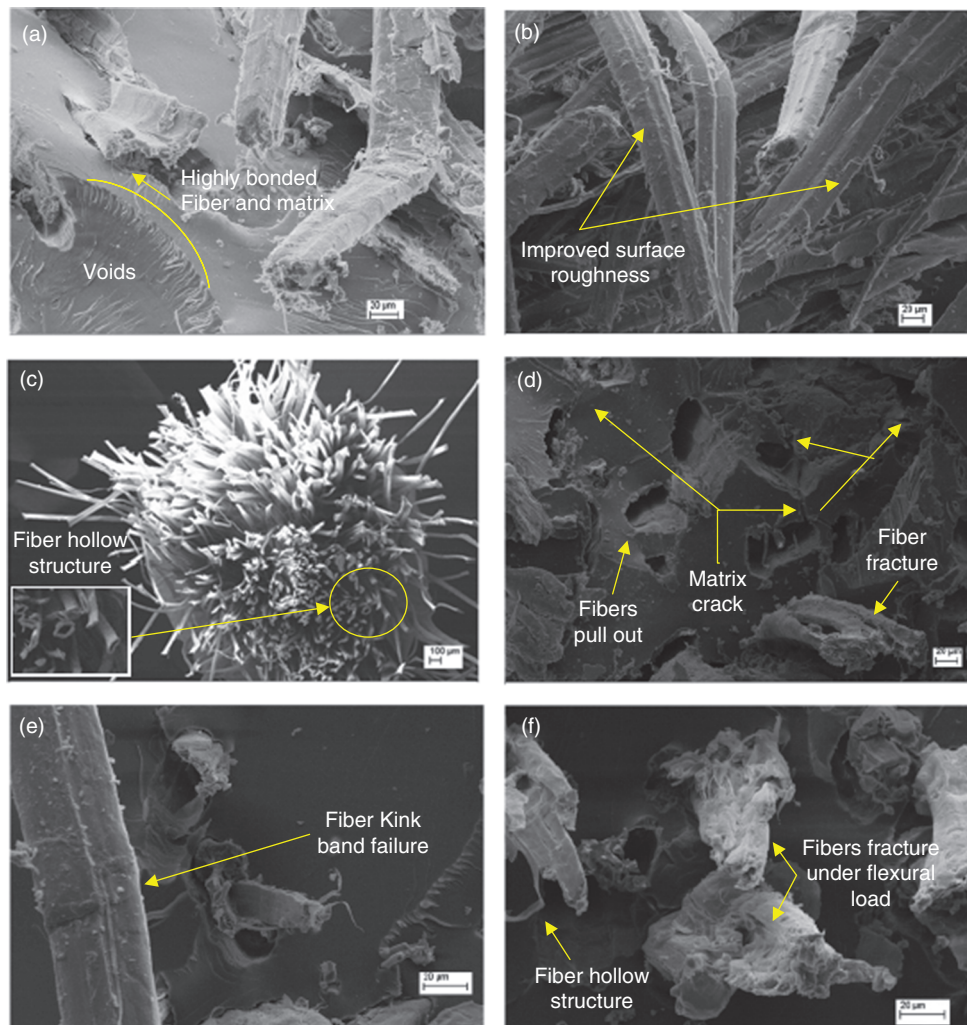


Fig. 1. (a) Fiber-matrix adhesion- $\times 20$, (b) Nettle fiber-surface modification- $\times 20$ and (c) Nettle fiber-hollow cross sectional view- $\times 100$, (d) Tensile test-fiber pull out and fracture,- $\times 20$, (e) Compression test Fiber-kink band failure,- $\times 10$, (f) Flexural test-Fiber fracture,- $\times 20$.

improved interface adhesion between fiber and matrix⁽¹⁷⁾ as shown in Figure 1(b) and also the random orientation of the nettle fiber in resin matrix can be clearly seen from the same figure. Figure 1(c) reveals the hollow structure of the nettle fiber. The hollow structure is expected to improve the specific stiffness and vibration absorption (damping) ability of the composite material.⁽¹⁸⁾ The fiber orientation decides the mechanical properties of the composite. The random orientation of the short fiber produced isotropic composite material which had properties that did not vary with direction.⁽¹⁹⁾ The random orientation helped to improve the resistance to slip (defect movement), thereby increasing the load carrying capacity of the material. Figure 1(a) shows the presence of voids in the form of air bubbles or air tunnels. The main cause for the void formation is high exothermic temperature produced by the addition of excess accelerator and catalyst for quick curing.

3. RESULTS

3.1. Mechanical and Dynamic Properties

3.1.1. Tensile Strength

Tensile test was carried out on a computerized (Zwick-Roell) universal testing machine as per ASTM D3039 standard with a flat specimen of size $250 \times 25 \times 2.5$ mm at standard laboratory atmosphere ($23 \text{ }^\circ\text{C} \pm 3 \text{ }^\circ\text{C}$ and $50 \pm 10\%$ relative humidity). The specimen was clamped using wedge grips at a grip length of 45 mm on each side. A gauge length of 150 mm and cross head speed of 2 mm/min was used for tensile strength measurement. The tests were conducted on 20 samples and the average values and standard deviation results are reported. From the failed specimens of tensile tested composite samples, two common types of failure were identified; LGM (lateral gage middle) and AGM (angled gage middle), representing failure type, area and location respectively. Figure 2(a) shows the test results as tensile stress in (MPa) versus elongation

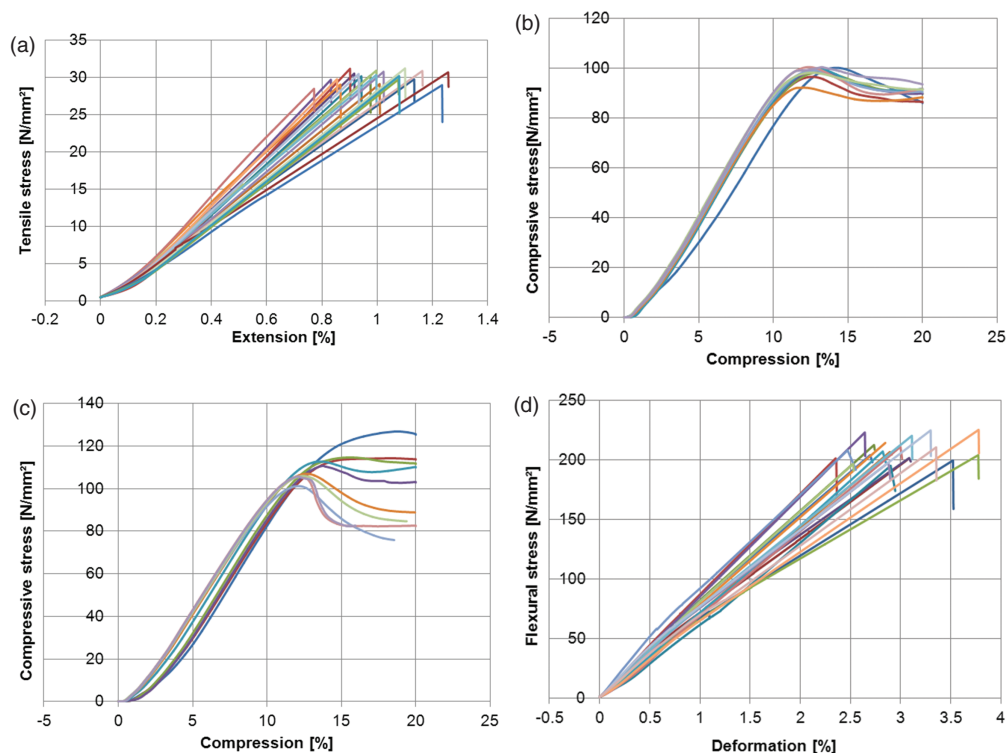


Fig. 2. (a) Tensile stress versus Extension plot (tensile test), (b) compressive stress versus deformation plot (test method-1, compressive load parallel to lay up direction) (c) compressive stress versus Deformation plot (test method-2, compressive load normal to lay up direction), and (d) flexural stress versus deformation plot (four point flexural test).

Copyright: American Scientific Publishers

in (%). The average tensile strength was observed as 30 ± 0.8 MPa at $1.0 \pm 0.1\%$ extension with the average elastic modulus being 2.936 ± 0.396 GPa.

3.1.2. Compressive Strength

Compression test was carried out on computerized (Zwick-Roell) universal testing machine as per ASTM D695 standard with the cubic specimen of size $25.4 \times 25.4 \times 25.4$ mm at standard laboratory atmosphere ($23 \text{ }^\circ\text{C} \pm 2 \text{ }^\circ\text{C}$ and $50 \pm 5\%$ relative humidity). The specimen was placed between the top and bottom jaws of the hardened compression base and cross head speed of 1.3 mm/min was used for compressive strength measurement. The tests were conducted on 20 samples and the average values and standard deviation results are reported. Figures 2(b) and (c) show the results as compressive stress in (MPa) versus compression in (%) for the applied load conditions of parallel and normal-to-fiber and matrix layup (stacking) direction. Average compressive strength of 98.5 ± 2.5 MPa at $13 \pm 0.5\%$ compression (parallel) and 110 ± 7 MPa at $14 \pm 2.5\%$ compression (normal) were observed.

3.1.3. Flexural Strength

The four point flexural test was carried out on a computerized (Zwick-Roell) universal testing machine as per ASTM D6272 standard with a flat specimen of size

$125 \times 12.7 \times 3.2$ mm at standard laboratory atmosphere ($23 \text{ }^\circ\text{C} \pm 2 \text{ }^\circ\text{C}$ and $50 \pm 5\%$ relative humidity). The specimen was supported and loaded by two steel hardened cylindrical rollers of same radius and geometry. The roller position and alignment were controlled with the help of alignment gauge and cross head speed of 1.4 mm/min was used for flexural strength measurement. The tests were conducted on 20 samples and the average values and standard deviation results are reported. From the failed specimens of flexure tested composite samples, two common types of failure were identified; TAT (tension, at loading nose, top) and TBM (tension, between loading noses, middle) representing failure mode, area and location respectively. Figure 2(d) shows the test results as flexural stress in (MPa) against deformation in (%). The average flexural strength was obtained as 208 ± 9.5 MPa at $3 \pm 0.4\%$ deformation.

Figures 2(a)–(d) show tensile, compression (normal, parallel) and flexural test results plot for nettle fiber reinforced-polyester resin matrix composite at 38% of fiber loadings.

3.2. Analytical Models for Tensile Properties

The development of mathematical models for the prediction of mechanical properties through the use of ROM has been widely reported in literature. By using such models, the conduct of costly and time consuming experiments can

be avoided. These models should be accurate and have to be validated in order to use it reliably.

3.2.1. Parallel Model

The parallel ROM is also called a uniform strain model⁽²⁰⁾ and is used to determine the Young's modulus (E_c) and tensile strength (σ_c) of composites in which fibers are oriented along the direction of loading. Equation (12) represents the parallel rule of mixture (ROM) used to predict the elastic modulus.

$$E_c = V_f \times E_f + V_m \times E_m \quad (12)$$

3.2.2. Series Model

The series model is also called a uniform stress model⁽²⁰⁾ and is used to determine the Young's modulus and tensile strength of composites in which fibers are oriented perpendicular to the direction of loading. The Eq. (13) for predicting the elastic modulus according to this model is given by,

$$E_c = \frac{E_f \times E_m}{V_f \times E_m + V_m \times E_f} \quad (13)$$

3.2.3. Hirsch's Model

The Hirsch's model is a combination of series model and parallel model and is used for determining the properties of composites with randomly oriented fibers. Equation (14) represents the Hirsch's model of ROM's. The coefficient x varies from 0 to 1 which is an indication of the, stress transfer between the fibers and the matrix.⁽²¹⁾

$$E_c = x \times (V_f \times E_f + V_m \times E_m) + (1-x) \times \frac{E_f \times E_m}{V_f \times E_m + V_m \times E_f} \quad (14)$$

3.2.4. Proposed Model

Equation (15) is the modified parallel ROM developed by Sreekumar et al.⁽¹⁵⁾ by adding an additional coefficient η to account for the weakening of composite due to the fiber orientation in parallel ROM Eq. (12). The coefficient η varies between 0 and 1, with 1 representing fiber orienting along the loading direction.

$$E_c = \eta \times V_f \times E_f + V_m \times E_m \quad (15)$$

Lamy and Baley⁽¹²⁾ adopted the parallel model and modified it to include the effect of fiber diameter in the composite. The effect of fiber orientation was not included in their work.

In this work, three new models (Model-1, Model-2 and Model-3) are developed to predict the tensile properties of the composite by ROM, by modifying the parallel, series and Hirsch's models respectively, to include the effects of both fiber orientation and variation in fiber diameters.

The modified parallel model (model-1) represented in Eq. (16) includes the effect of variation in fiber diameters

in the model developed by Sreekumar et al.⁽¹⁵⁾ The variation in fiber diameter is accounted by considering the contribution of Young's modulus of fibers of each class i in the calculation of Young's modulus of composite and hence, this equation is likely to make more accurate predictions.

$$E_c = \eta \left\{ \left(\sum_{i=1}^n n_i \times 0.55 d o_i^2 \right) \times \left(\frac{\sum_{i=1}^n n_i \times 0.55 d o_i^2}{\sum_{i=1}^n n_i \times 0.55 d o_i^2} \times E_i \right) \right\} + \left\{ \left(1 - \sum_{i=1}^n n_i \times 0.55 d o_i^2 \right) \times E_m \right\} \quad (16)$$

Equation (17) is the modified series model (model-2) which includes the effect of both fiber orientation and variation in fiber diameters in the series model.

$$E_c = \left(\left(\frac{\sum_{i=1}^n n_i \times 0.55 d o_i^2}{\sum_{i=1}^n n_i \times 0.55 d o_i^2} \times E_i \right) \times E_m \right) \times \left(\left(\sum_{i=1}^n n_i \times 0.55 d o_i^2 \right) \times E_m \right) + \left(\frac{\sum_{i=1}^n n_i \times 0.55 d o_i^2}{\sum_{i=1}^n n_i \times 0.55 d o_i^2} \times E_i \right) - \eta \left\{ \left(\sum_{i=1}^n n_i \times 0.55 d o_i^2 \right) \times \left(\frac{\sum_{i=1}^n n_i \times 0.55 d o_i^2}{\sum_{i=1}^n n_i \times 0.55 d o_i^2} \times E_i \right) \right\}^{-1} \quad (17)$$

Equation (18) is the modified Hirsch's model (model-3) which combines the modified parallel and modified series model.

$$E_c = x \times \left\{ \left(\sum_{i=1}^n n_i \times 0.55 d o_i^2 \right) \times \left(\frac{\sum_{i=1}^n n_i \times 0.55 d o_i^2}{\sum_{i=1}^n n_i \times 0.55 d o_i^2} \times E_i \right) \right\} + \left\{ \left(1 - \sum_{i=1}^n n_i \times 0.55 d o_i^2 \right) \times E_m \right\} + (1-x) \times \left(\left(\frac{\sum_{i=1}^n n_i \times d o_i^2}{\sum_{i=1}^n n_i \times d o_i^2} \times E_i \right) \times E_m \right) \times \left(\left(\sum_{i=1}^n n_i \times 0.55 d o_i^2 \right) \times E_m \right) + \left(\frac{\sum_{i=1}^n n_i \times d o_i^2}{\sum_{i=1}^n n_i \times d o_i^2} \times E_i \right) - \eta \left\{ \left(\sum_{i=1}^n n_i \times 0.55 d o_i^2 \right) \times \left(\frac{\sum_{i=1}^n n_i \times 0.55 d o_i^2}{\sum_{i=1}^n n_i \times 0.55 d o_i^2} \times E_i \right) \right\}^{-1} \quad (18)$$

Similarly, the modified parallel, series and Hirsch's model (model 1, 2 and 3) for tensile strength are given by Eqs. (19)–(21) respectively.

$$\sigma_c = \eta \left\{ \left(\sum_{i=1}^n n_i \times 0.55 d o_i^2 \right) \times \left(\sum_{i=1}^n \frac{n_i \times 0.55 d o_i^2}{\sum_{i=1}^n n_i \times 0.55 d o_i^2} \times \sigma_i \right) \right\} + \left\{ \left(1 - \sum_{i=1}^n n_i \times 0.55 d o_i^2 \right) \times \sigma_m \right\} \quad (19)$$

$$\sigma_c = \left(\left(\sum_{i=1}^n \frac{n_i \times 0.55 d o_i^2}{\sum_{i=1}^n n_i \times 0.55 d o_i^2} \times \sigma_i \right) \times \sigma_m \right) \times \left(\left(\sum_{i=1}^n n_i \times 0.55 d o_i^2 \right) \times \sigma_m \right) + \left(\sum_{i=1}^n \frac{n_i \times 0.55 d o_i^2}{\sum_{i=1}^n n_i \times 0.55 d o_i^2} \times \sigma_i \right) - \eta \left\{ \left(\sum_{i=1}^n n_i \times 0.55 d o_i^2 \right) \times \sum_{i=1}^n \frac{n_i \times 0.55 d o_i^2}{\sum_{i=1}^n n_i \times 0.55 d o_i^2} \times \sigma_i \right\}^{-1} \quad (20)$$

$$\sigma_c = x \times \left\{ \left(\sum_{i=1}^n n_i \times 0.55 d o_i^2 \right) \times \left(\sum_{i=1}^n \frac{n_i \times 0.55 d o_i^2}{\sum_{i=1}^n n_i \times 0.55 d o_i^2} \times \sigma_i \right) \right\} + \left\{ \left(1 - \sum_{i=1}^n n_i \times 0.55 d o_i^2 \right) \times \sigma_m \right\} + (1-x) \times \left(\left(\sum_{i=1}^n \frac{n_i \times d o_i^2}{\sum_{i=1}^n n_i \times d o_i^2} \times \sigma_i \right) \times \sigma_m \right) \times \left(\left(\sum_{i=1}^n n_i \times 0.55 d o_i^2 \right) \times \sigma_m \right) + \left(\sum_{i=1}^n \frac{n_i \times d o_i^2}{\sum_{i=1}^n n_i \times d o_i^2} \times \sigma_i \right) - \eta \left\{ \left(\sum_{i=1}^n n_i \times 0.55 d o_i^2 \right) \times \sum_{i=1}^n \frac{n_i \times 0.55 d o_i^2}{\sum_{i=1}^n n_i \times 0.55 d o_i^2} \times \sigma_i \right\}^{-1} \quad (21)$$

where η , x -orientation and stress transfer coefficients.

For better correlation between the analytical and experimental results, the values of x and η were varied between the limits and investigations were carried out.

4. DISCUSSION

4.1. Tensile Strength

Figure 3 and Table IV show the comparison of theoretical and experimental Young's modulus (E_c) and (σ_c) tensile strength of the composite obtained using the models developed. In the case of Young's modulus, both modified parallel model (model-1) and modified Hirsch's model

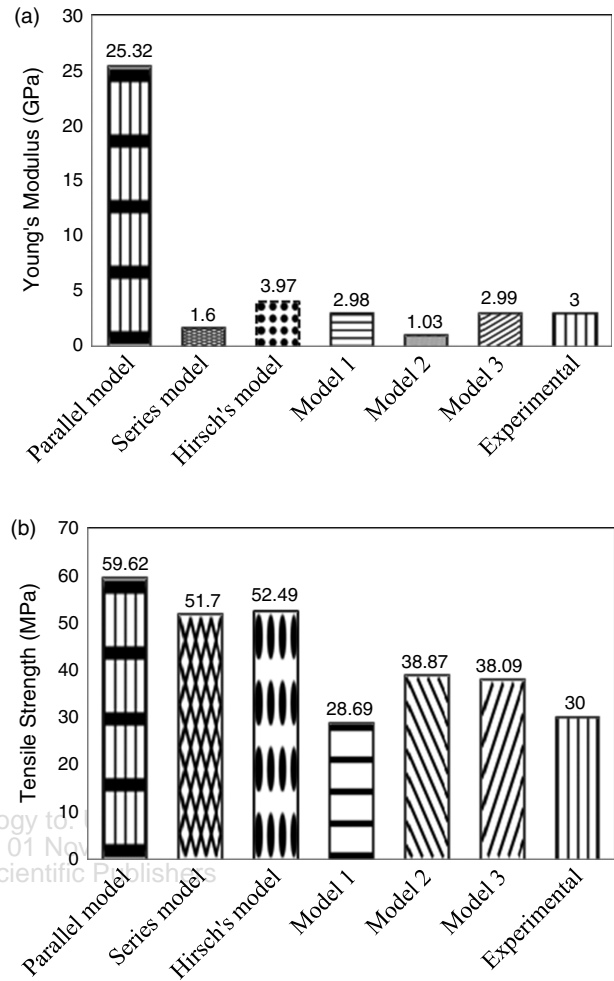


Fig. 3. Comparison of analytical and experimental tensile properties of nettle fibers. (a) Young's modulus (b) Tensile strength.

(model 3) are in good correlation with the experimental value with $\eta = 0.1$ and $x = 0.1$ and the corresponding deviations were found to be only 0.666% and 0.333% respectively. This implies that the short nettle fibers are randomly oriented rather than being oriented along the tensile load direction.^(15,20) The value of x is found to be low, which indicates that the bonding strength (mechanical interlocking between fiber and matrix) is affected by the presence of voids and fiber surface irregularities. But the modified series model (model-2) deviated drastically from the experimental value. Similarly, in the case of tensile

Table IV. Comparison of analytical and experimental Young's modulus and Tensile strength at $\eta = 0.1$ and $x = 0.1$.

Model	Experimental $E = 3$ GPa		Experimental $\sigma = 30$ MPa	
	E (GPa)	Deviation (%)	Model	σ (MPa)
1	2.98	0.6667	1	28.69
2	1.03	65.6667	2	38.87
3	2.99	0.3333	3	38.09

strength, modified parallel model (model-1) showed good correlation with the experimental value with a deviation of 4.366%, while the other two models had a deviation of more than 26%.

Figure 4 is the schematic diagrams illustrating various failure modes of composite material when subjected to tensile load like matrix crack propagation and matrix crack and fiber fracture.

During initial loading, the micro cracks which had been already present in the matrix due to residual thermal stress⁽²²⁾ were enlarged. In a fiber, lignin and hemicellulose are present in the primary wall crystalline cellulose microfibrils network. Cellulose, hemicellulose and lignin with pectin act as bonding agent⁽³⁾ and hold the microfibrils in position and resist slip formation up to some extent of tensile loading. But a treatment with higher content of NaOH (8 and 10%) causes extensive removal of lignin and hemicelluloses.⁽¹¹⁾ Due to this, the binding effect is reduced and this influences lateral contraction and easy microfibrils deformation. This reduces the frictional resistance of microfibrils and de-bonding of fiber from matrix is initiated as shown in Figure 1(d). Due to the presence of voids in the matrix, the cracks suddenly propagated. Then, the sample fractured at a stress far below the yield strength. This could be because stress concentration at polymer voids (air bubbles or air tunnel) initiated matrix shear or crack

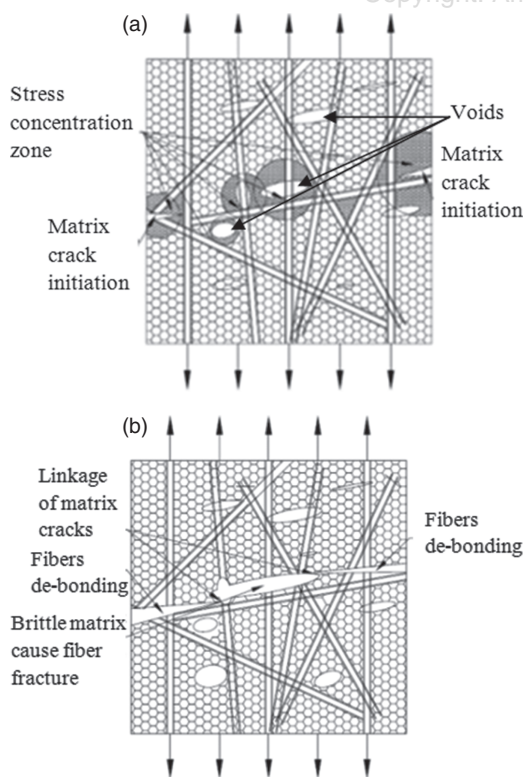


Fig. 4. Schematic diagrams showing the formation of failure modes of tensile test. (a) Matrix crack propagation, and (b) matrix crack and fiber fracture.

in matrix material by nucleating the voids,⁽²³⁾ that grew and linked, ultimately causing crack at different locations and at different angles. Further, incremental tensile load in the composite caused the fibers to get debonded from the matrix and as a result of it they were pulled out easily from matrix resulting in fracture which resulted in the lower tensile properties of the composite. The result shows that the composite was weaker in shear than in tension at maximum loads, because slip was developed along the plane of maximum shear stress 45° and cause fiber fracture (shear failure) with respect to longitudinal axis of the tensile specimen. This is an interfacial failure, which results in loss of surface smoothness and defibrillation of the fiber.⁽²¹⁾ This is an evidence to show that the composite behaviour is ductile in nature. Epaarachchi et al.⁽²⁴⁾ and Sathishkumar et al.⁽²⁵⁾ observed the similar trend in experimental tensile modulus and strength for cotton-vinylester and snake grass-polyester composite respectively.

4.2. Compressive Strength

Two compressive tests were conducted as per ASTM D695 standard; the compressive load was applied parallel and normal to fiber and matrix layup direction. In the first test method, the major failure modes are elastic-micro buckling of fibers—kink band, pure compressive failure and shear failure in fiber.⁽²⁶⁾ Figure 5 shows schematic diagrams of sequential formation of kinking failure mode.

When the specimen was subjected to axial compressive load, elastic micro buckling failure mode of the fibers oriented along the loading direction was observed. On increasing the load, matrix strength and hardness prevented fiber bending⁽²⁷⁾ as the matrix tends to started yielding by strain hardening effect. Moreover, there was no further increase in stress, but there was an increase in strain. Further incremental loading locally initiated fiber fracture because of insufficient lateral support of fiber and poor fiber–matrix interfacial bonding strength at matrix free-edge region, voids in matrix and also micro crack defects present in the fiber. Finally, the random fibers in the composite specimen fractured, due to the development of matrix cracks after matrix yielding and excessive bending during micro buckling⁽²⁷⁾ as shown in Figure 1(e). Now, it lost its structural integrity and the specimen collapsed. Bartosz et al.⁽²⁸⁾ observed the similar kind of failure mechanism and experimental compressive strength in hemp-polyester composite.

In the second compression test method, the loading direction is normal to fiber and matrix layup direction. The major failure modes were lateral contraction of fibers, barrel formation and crushing failure mode. Figure 6 shows the sequential failure modes in the second compression test method.

The normally aligned fiber and matrix layer, when subjected to initial compressive load exhibited lateral contraction of fibers and matrix yielding. Further incremental loading caused an increase in strain but not in

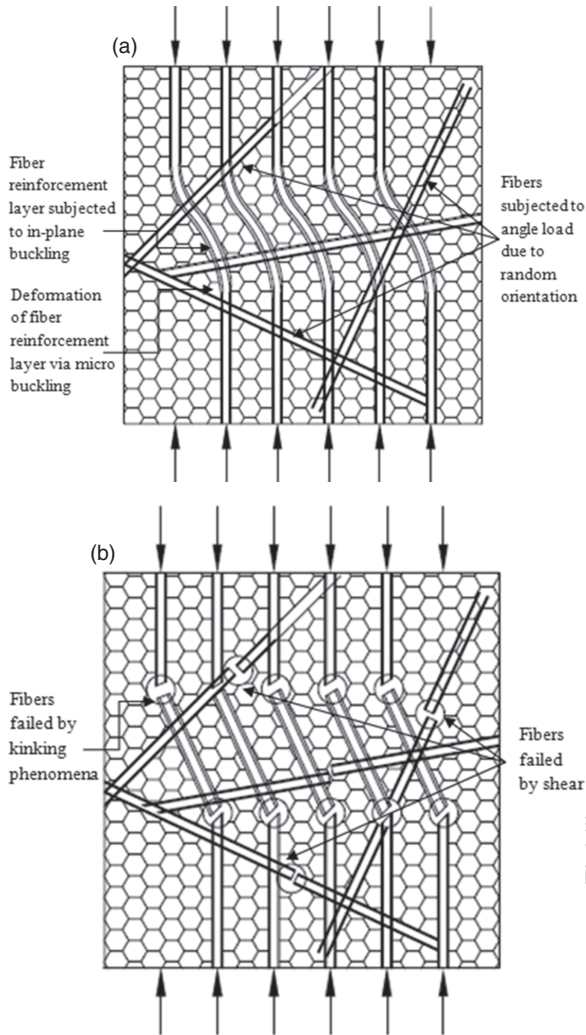


Fig. 5. Schematic diagrams showing the formation of failure modes of compression test (parallel). (a) In-plane buckling of fibers layers cause deformation of fibers via micro buckling and (b) fibers kinking phenomena and shear causing catastrophic failure.

stress. The matrix started to yield by strain hardening effect and transverse cracks on matrix were initiated. The high extensibility and toughness which are inherent properties of the nettle fiber make it withstand the stress applied and prevent catastrophic failure of the composite.⁽²¹⁾ It is evident from the stress–strain curve obtained in the compression test and is shown in Figure 2(c). After the shear failure of the matrix, the fiber de-bonded from it and was subjected to bending load. It produced compressive and tensile stresses on the inner and outer surfaces of the fiber, thereby initiating fiber shear. At the same time, highly compressed, failed and brittle micro-particles of the matrix helped to increase this fiber shear rate. Now, the composite specimen entered into crushing failure mode due to higher fiber volume packing, because of the accumulation of failed fibers and failed brittle micro-particles of matrix over one another. Thus,

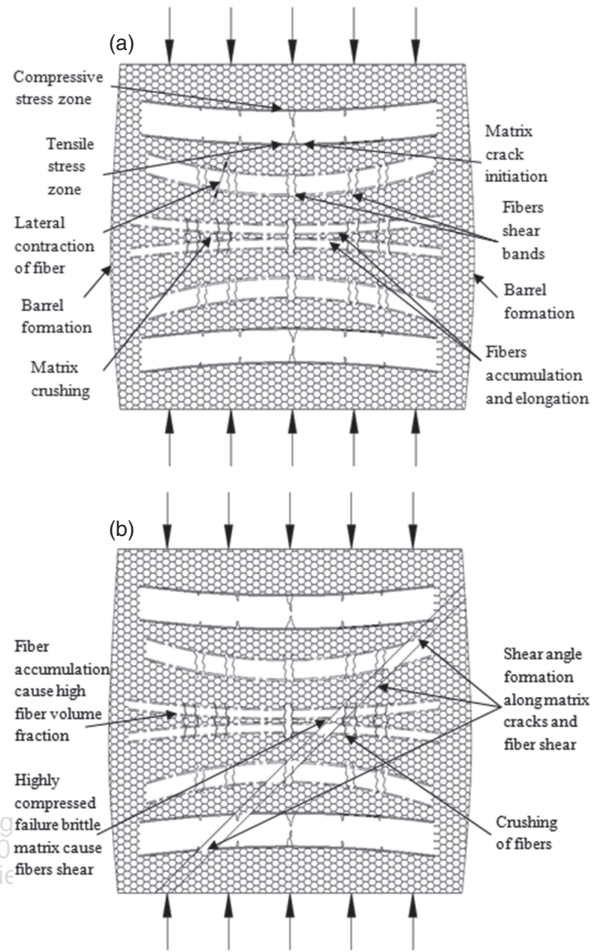


Fig. 6. Schematic diagrams showing the formation of failure modes of compression test (normal). (a) Lateral contraction of fibers cause barrel formation and (b) Crushing failure mode.

normal compressive testing condition yield higher compressive strength than parallel compressive testing condition as shown in Figures 2(b), (c).

4.3. Flexural Strength

The supporting span-to-depth ratio of 16:1 is chosen for four point flexural test. Flexural strength is the stress in the outer most fiber at convex side of the composite specimen. Tensile stress on the convex side and compression stress on the concave side create shear stress on the middle portion of the specimen. To find whether the primary failure occurred due to tension or compression stress, the shear stress should be minimized. In a three-point flexural test, the area of uniform stress is small and hence concentrated load acts below the center loading point producing shear failure at specimen. But, in a four-point flexural test, the area of uniform stress exists between the inner span loading points which reduces shear failure. The major failure modes are matrix cracks and fiber fragmentation on tensile stress surface. Figure 7 shows schematic diagrams of sequential failure modes of flexural test.

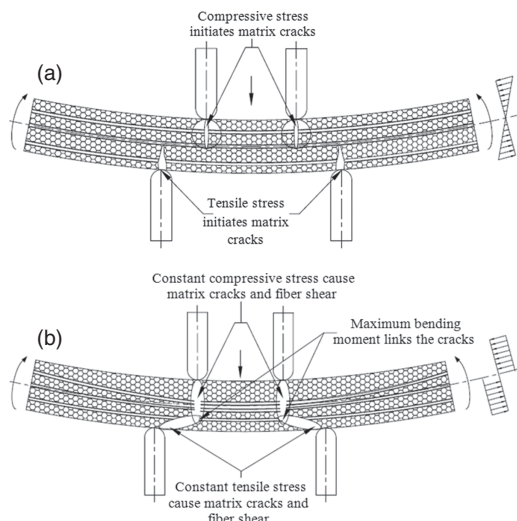


Fig. 7. Schematic diagrams showing the formation of failure mode. (a) Matrix cracks. (b) Fibers fragmentation.

Since the reinforcing material (nettle fiber) has a hollow structure by nature as shown in Figures 1(c), (f) the composite exhibits more bending stiffness and specific rigidity.⁽¹⁸⁾ At initial load quasi-linear part reveals that the matrix started to yield by strain hardening effect and transverse cracks were initiated on it. This shows that there was no further increase in stress but there is an increase in strain and thereby influencing the fiber shear after matrix yielding. Also, the randomly dispersed short nettle fibers helped to bridge the voids in the matrix and reduced micro crack propagation rate in the matrix at the maximum bending stress. Further incremental load caused a small crack zone formation due to fiber elongation and de-bonding at the outer surface, where the stress was maximum. Moreover, as the bending moment increased, the crack zone grew inwards from the surface, and at the maxima, the crack zone penetrated through the section of the beam by

matrix crack linkage. The brittle matrix underwent shear failure at the fiber matrix interface. Now the failure was caused by constant compressive and tensile stress distribution on the entire cross sectional area of the specimen.⁽²³⁾ As a result, fracture developed along the matrix cracks and fiber shear zones producing fiber fragmentation failure mode and then finally fail catastrophically. The composite prepared by compression moulding process at a fiber volume fraction of 38% shows maximum flexural strength, Sreekumar et al.⁽¹⁵⁾ and Sathishkumar et al.⁽²⁵⁾ reported similar results in sisal-polyester and snake grass-polyester composite respectively.

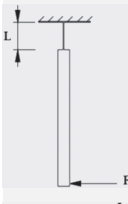
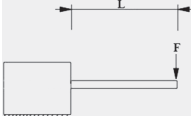
4.4. Free Vibration Modal Analysis

The dynamic characteristics of the composite cantilever beam specimen were obtained by impulse dynamic test. To measure material and structural damping ratio, time domain data and frequency domain data were recorded using LabVIEW software, DAQ (NI 9234) and the accelerometer-(DYTRAN3097A2, sensitivity 96.72 mV/g) mounted on the top of the composite beam using bee wax. The impact force was applied with the help of impact hammer to excite the beam. The damping ratios (ζ) were estimated using the half power bandwidth method⁽²⁹⁾ using the Eq. (22).

$$\zeta = \frac{f_2 - f_1}{2f_n} \quad (22)$$

Here $f_2 - f_1$ and n, f_n represent half power band width and the corresponding frequency, respectively. The natural frequencies of the beam material and structural modes along with the corresponding damping ratios are listed in Table V. It can be observed that the cantilever beam composite specimen has a large material damping ratio at fundamental natural frequency. Its value was found to be in the (order 10^{-1}) range of 0.35 to 0.45, which was associated with its fundamental natural frequency of 20.507 Hz. At higher frequencies, the damping ratio was found to be

Table V. Dynamic characteristics of the cantilever beam composite specimen obtained by impulse dynamic test.

Test configuration	Hanging/overhanging distance (mm)	Mode 1		Mode 2	
		Natural frequency (Hz)	Damping ratio	Natural frequency (Hz)	Damping ratio
Material damping					
	100	20.507	0.442	78.125	0.039
	200	20.507	0.422	78.125	0.024
	300	20.507	0.414	77.148	0.022
Material + Structural damping					
	250	19.531	0.427	59.57	0.036
	350	28.32	0.053		
	450	17.578	0.032		

in the (order 10^{-2}) range of 0.02 to 0.04 and the corresponding frequency was found to be 78.125 Hz. Similarly, for structural damping, the damping ratios were found to be in the (order 10^{-2}) range of 0.05 to 0.08. It can be observed that, in structural damping, as overhanging distance varies, the natural frequency and damping ratio varies. At higher frequencies, the average damping ratio was found to be 4 to 10 times higher for short randomly oriented nettle fiber–polyester resin matrix composite than the other materials reported by Emmanuil et al.⁽³⁰⁾ The cross section of nettle bio-fiber stem is hollow, unlike flax and many other bast fibers.⁽³¹⁾ This unique morphology of nettle fiber enables it to absorb more vibration and exhibit improved damping properties. Unlike continuous fiber, the short fiber did not directly carry the externally applied loads.⁽²⁵⁾ The externally applied load was first carried by the matrix and then it was transferred onto the random short fibers via the fiber ends and the surfaces of fibers. The short fiber also enhances interface thickness and stiffness by increasing the surface to contact area between fiber and matrix. This phenomenon helped to enhance the damping property of the composite material.⁽³²⁾ The viscoelastic nature of resin also leads to higher damping.⁽³³⁾ Additionally, the matrix part of the polymer molecular chains could slide and rearrange to dissipate the energy, which also enhanced the damping ratio. Senthilkumar et al.⁽³¹⁾ reported similar results in banana–polyester and sisal–polyester composite respectively.

5. CONCLUSION

Characterization of the mechanical and dynamic properties of randomly oriented short nettle fiber reinforcement–polyester resin matrix composite was carried out. The random orientation of the fiber produced isotropic composite material, which has properties that do not vary with direction within the composite material.

The tensile test carried out as single himalayan nettle (*Girardinia heterophylla*) fiber revealed the effective Young's modulus (E_i) and tensile strength (σ_i) depends on fiber diameters (d_{o_i} , d_{i_i}) and decrease with increase in fiber diameter. The chemical composition test reported that the fiber has higher content of cellulose, hemicellulose and lignin, which yields better mechanical properties and thermal stability. The density of nettle fiber is 1230 kg/m³ which is lower than that of other fibers and hence it yields higher specific strength.

The morphological analysis (SEM) showed that the nettle fiber is hollow unlike flax and other bast fibers; a good interfacial bonding between the fiber and the matrix was also observed.

Three analytical models were developed based on ROM for the prediction of tensile properties. The newly proposed parallel model (model 1) had better correlation with experimental values at $\eta = 0.1$ and $x = 0.1$ which implies that the short nettle fibers are randomly oriented rather than

being oriented along the tensile load direction for better stress transfer in fiber and matrix.

Damping ratio was estimated based on half power bandwidth method from the results of modal analysis. It can be observed that the cantilever beam composite specimen has large material and structural damping ratio at fundamental natural frequency. The hollow nature of the nettle fiber enhanced vibration absorption and the matrix part of polymer molecular chains could slide and rearrange to dissipate the energy and exhibited improved damping properties when subjected to an impulse force.

The aim of the study was to explore the suitability of the developed composite for structural applications, particularly, machine tools. One of the major requirements for machine tools to operate at high speeds is high damping. The investigations revealed that the newly developed composite exhibits better damping ratio. At higher frequencies, the (order 10^{-2}) the average damping ratio was found to be 4 to 10 times higher for short randomly oriented nettle fiber–polyester resin matrix composite than cast iron and epoxy granite. This shows that the new material can be considered as a candidate material for precision machine tools, aero-space, automobile and other structural applications.

Acknowledgments: We express our sincere thanks to the Principal, PSG College of Technology and the Head, PSG Techs COE Indu Tech Coimbatore, for providing basic laboratory and testing facilities.

References and Notes

1. R. M. Rowell, A. Sanadi, R. Jacobson, and D. Caulfield; Properties of kenaf/polypropylene composites; Kenaf Properties, Processing and Products; Mississippi State University Press, Mississippi State, MS (1999), pp. 381–392.
2. A. K. Mohanty, M. Misra, and L. T. Drzal; Sustainable bio composites from renewable resources: Opportunities and challenges in the green materials world; *J. Polym. Environ.* 10, 19 (2002).
3. J. Summerscales, P. J. Nilmini Dissanayake, S. Amandeep Virk, and W. Hall; A review of bast fibres and their composites part 1—Fibres as reinforcements; *Composites Part A* 41, 1329 (2010).
4. T. Nishino, K. Hirao, M. Kotera, K. Nakamae, and H. Inagaki; Kenaf reinforced biodegradable composite; *Compos. Sci. Technol.* 63, 1281 (2003).
5. S. Ochi; Mechanical properties of kenaf fibers and kenaf/PLA composites; *Mech. Mater.* 40, 446 (2008).
6. K. Goda, M. S. Sreekala, A. Gomes, T. Kaji, and J. Ohgi; Improvement of plant based natural fibers for toughening green composites—effect of load application during mercerization of ramie fibers; *Composites Part A* 37, 2213 (2006).
7. E. Bodros and C. Baley; Study of the tensile properties of stinging nettle fibres (*Urtica dioica*); *Mater. Lett.* 62, 2143 (2008).
8. A. S. Singha and Vijay Kumar Thakur; Mechanical properties of natural fiber reinforced polymer composites; *Bull. Mater. Sci.* 31, 791 (2008).
9. Y. Xie, A. S. Hill Callum, Z. Xiao, Z. Xiao, H. Militz, and C. Mai; Silane coupling agents used for natural fiber/polymer composites: A review; *Compos. Part A* 41, 806 (2010).
10. A. Athijayamani, M. Thiruchitrambalam, V. Manikandan, and B. Pazhanivale; Mechanical properties of natural fibers reinforced polyester hybrid composite; *Int. J. Plast Technol.* 14, 104 (2010).

11. M. M. Kabir, H. Wang, K. T. Lau, and F. Cardona; Tensile properties of chemically treated hemp fibres as reinforcement for Composites; *Composites Part B* 53, 362 (2013).
12. B. Lamy and C. Baley; Stiffness prediction of flax fibers-epoxy composite materials; *J. Mater. Sci. Lett.* 19, 979 (2000).
13. M. Zimulewska, M. WladykaPrzybylak, and J. Mankowski; Cellulosic bast fibers, their structure and properties suitable for composite applications; In *Cellulose Fibers: Bio and Nano-Polymer Composites*, Springer-Verlag, Berlin, Heidelbergpp (2011), pp. 98–117.
14. A. S. Singha and Vijay Kumar Thakur; *Green Polymer Materials*, Studium Press LLC, USA (2012).
15. P. A. Sreekumar, K. Joseph, G. Unnikrishnan, and S. Thomas; A comparative study on mechanical properties of sisal-leaf fibre-reinforced polyester composites prepared by resin transfer and compression moulding techniques; *Compos. Sci. Technol.* 67, 453 (2007).
16. X. Li, G. Lope Tabil, and Satyanarayan Panigrahi; Chemical treatments of natural fiber for use in natural fiber-reinforced composites: A review; *J. Polym. Environ.* 15, 25 (2007).
17. G. Bogoeva-Gaceva, M. Avella, M. Malinconico, A. Buzarovska, A. Grozdanov, G. Gentile, and M. E. Errico; Natural fiber eco composites; *Polym. Compos.* 28, 98 (2007).
18. M. Hucker, I. Bond, S. Bleay, and S. Haq; Investigation into the behaviour of hollow glass fibre bundles under compressive loading; *Compos. Part A* 34, 1045 (2003).
19. J. Ever Barbero; *Introduction to Composite Materials Design*, Taylor & Francis Group, CRC Press, Boca Raton (2013).
20. J. M. Paulo Monteiro; A note on the Hirsch model; *Cem. Concr. Res.* 21, 947 (1991).
21. S. Joseph, M. S. Sreekala, Z. Oommen, P. Koshy, and S. Thomas; A comparison of the mechanical properties of phenol formaldehyde composites reinforced with banana fibres and glass fibres; *Compos. Sci. Technol.* 62, 1857 (2002).
22. F. L. Mathews and R. D. Rawlings; *Composite Materials: Engineering and Science*, Woodhead Publishing Limited, England (1994).
23. M. Ashby, H. Sherclif, and D. Cebon; *Materials Engineering, Science, Processing, and Design*, Elsevier, United Kingdom (2007).
24. J. Epaarachchi, H. Ku, and K. Gohel; A simplified empirical model for prediction of mechanical properties of random short fiber/vinyl ester composites; *J. Compos. Mater.* 44, 779 (2010).
25. T. P. Sathishkumar, P. Navaneethakrishnan, and S. Shankar; Tensile and flexural properties of snake grass natural fiber reinforced isophthalic polyester composites; *Compos. Sci. Technol.* 72, 1183 (2012).
26. A. Jumahat, C. Soutis, F. R. Jones, and A. Hodzic; Fracture mechanisms and failure analysis of carbon fibre/toughened epoxy composites subjected to compressive loading; *Compos. Struct.* 92, 295 (2010).
27. B. A. Muralidhar; Tensile and compressive behaviour of multilayer flax-rib knitted preform reinforced epoxy composites; *Mater. Des.* 49, 400 (2013).
28. T. B. Weclawski, M. Fan, and D. Hui; Compressive behaviour of natural fibre composite; *Composites Part B* 67, 183 (2014).
29. S. S. Rao; *Mechanical Vibrations*; Pearson Education, India (2009).
30. E. F. Kushnir, Mahendra R. Patel, and T. M. Sheehan; Material considerations in optimization of machine tool structure, *ASME International Mechanical Engineering Congress and Exposition*, New York, NY, November (2001).
31. Y. Claire Barlo and D. Neal (eds.); *Fiber from Stinging Nettles*, Poster Presentation in Institute for Manufacturing, Cambridge University, United Kingdom, November (2011).
32. K. Senthil Kumar, I. Siva, P. Jeyaraj, J. T. Winowlinjappes, S. C. Amico, and N. Rajini; Synergy of fiber length and content on free vibration and damping behavior of natural fiber reinforced polyester composite beams; *Mater. Des.* 56, 379 (2014).
33. R. Chandra, S. P. Singh, and K. Gupta; Damping studies in fiber-reinforced composites—A review; *Compos. Struct.* 46, 41 (1999).

Received: 7 August 2014. Revised/Accepted: 1 June 2015.